R/S Analysis in LHD Filament Ejection Pattern

D. Carralero[1], M. Shoji[2], E. de la Cal[1], I. Calvo[1], J.L. de Pablos[1], C. Hidalgo[1] and H. Yamada[2]

[1]*Laboratorio Nacional de Fusión, EURATOM-CIEMAT, Madrid, Spain*

[2]*National Institute for Fusion Science, Toki, 509-5292, Japan*

During 2009 and 2010 experimental campaigns, LHD high β plasmas were observed by a fast camera (a non-line filtered Photron APX-RS capable of 200 kHz operation, coupled to a 75 mm objective) placed on 6-T tangential port, overlooking a region of almost 90º of the vacuum vessel. Figure 1 shows the general experimental layout. Visible radiation detected by the camera is produced by line radiation of light elements (essentially Hα and C II), which takes place in relatively cold regions of the plasma (i.e., the edge). Typical SOL is usually under the so called "ionizing plasma edge conditions" (T_e under 100eV; $n_e \approx 10^{19} m^{-3}$ near the LCFS). In such conditions, the excitation rate is essentially constant and the signal can be regarded as proportional to ne and no in the point of emission, where no is the emitting element density. Interpretation of camera output is non trivial given the geometrical complexity and broad field of view (FOV), although several important features can be recognized (as highlighted in figure 2e): helicoidal illuminated curves correspond to the positions of the two X point regions. Between these and the bright curves on the wall indicating strike point regions (SP), the tenuous stripe of the divertor leg magnetic surface can be seen. This leg corresponds to the blue surface displayed in figure 2f, where magnetic lines outside the ergodic layer (the area without clear curves) are represented. Finally, the darkened region of figure 2e corresponds to the FOV of the camera for 50 kHz operation. Analyzed areas signal is emitted at quite well determined magnetic regions (either the X point or the divertor leg) which almost never overlap on the camera FOV, reducing greatly line integration effects and thus allowing to identify the 3D position from a 2D view. It must be noticed how the area of maximum emission near the X point does not correspond with the external region of the ergodic layer, as would be expected (see, e.g. [1], [2]), but it is shifted radially outwards some 15 cm. This can be explained as a result of the aforementioned increase of the ergodic layer width due to finite β. Moreover, a 15 cm shift is in very good agreement with HINT simulations in [3]. During high β discharges, filaments can be seen propagating along divertor leg surfaces both toroidally, along the direction of the magnetic field, and radially, alternating between inwards and outwards motion. Frequency spectra of the camera signals (sampled on the regions where filament activity is present, such as the red cross highlighted pixel in figure

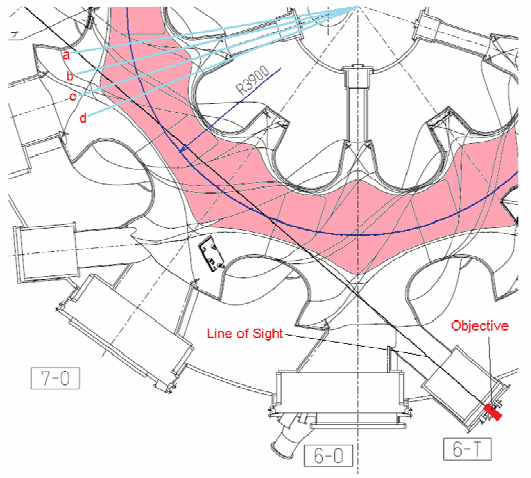

Fig. 1 *Equatorial plane top view. Observation port, line of sight and confined plasma region (purple) are displayed. Blue circumference is R = 3.9 m. Light blue lines show the perpendicular planes in figure 2*

2a) show a strong and well defined activity band in the range of 2-3.5 kHz and some "secondary" and sparser activity is found in the range of 4-10 kHz [4]. The very well defined frequency in the low band activity, suggests the possibility of a coherent source for it. Besides, its range of 2-3 kHz is very similar to the one associated to the m/n = 2/3 edge mode (dominant in these regime [3]) and magnetic probe spectral data shows a strong relation between the mode and low band activity [4]. However, "comet"-like filament activity (as seen in figure 3) on the 4-10 kHz range still retains a significative fraction of the spectral power but can not be easily related to a clear frequency band. This irregular ejection pattern suggests that effects other than MHD (most likely, turbulence related mechanisms) may be playing a relevant role on the generation of such filaments. In particular, long term correlation methods, searching memory effects along wide temporal sequences, seem especially well fitted to analysis this kind of stochastic process. This observation of stochastic, helically coherent and strongly pulsed macroscopic structures being ejected from the plasma edge towards the wall suggests the presence of avalanch-like phenomena, taking place either in the edge itself or in inner regions of the plasma. In such case, the bursted particle ejection would then cross the LCFS and ergodic layer to eventually be released on the wall through the divertor legs. The phenomenon of avalanches (i.e., well-differentiated, irregular structures of varying sizes) has been the subject of much study since the 90s. In particular, avalanches are a central element of the Self

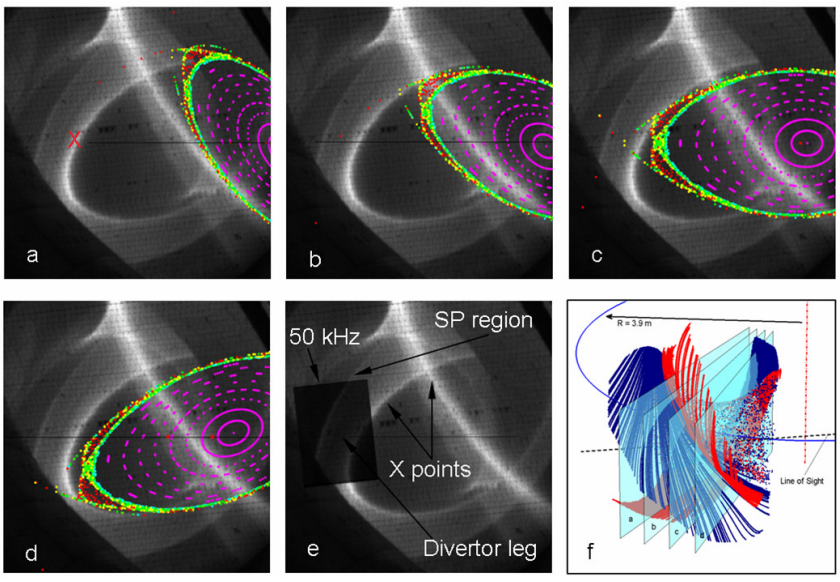

Fig. 2 *(a-d) Vacuum magnetic field lines in vertical planes of equal labels in fig 1. Horizontal black line represents equatorial plane. Color indicates connection length (Purple is confined plasma. (e) main features are highlighted. Shadowed area is 50 kHz operation FOV. (f) 3D geometry of divertor leg surfaces (in different colors for better perception).*

Organized Criticality (SOC) paradigm, in which turbulent processes are limited by local thresholds which can be fastly relaxed and interact between them [5,6], thus giving rise to avalanches. These SOC-generated events are characterized by their non-locality and multiscale nature, and specifically by the self-similarity of the fluctuations associated to them. Much work has been realized on this topic: On one hand SOC features (such as self-similarity and pulsed events) have been simulated on turbulent plasma physics numerical models, such as [7], in which a simplified model based in resistive pressure gradient driven (g-mode, present in LHD high β discharges [8]) turbulence was employed. On the other hand, several experiments have detected self-similar behaviour on the fluctuations (mostly floating potential, measured by Langmuir probes) of the boundary regions of a number of tokamaks (JET, DIIID, TJ-I) and stellarators (W-7AS, TJ-IU, ATF) [9,10]. A widely extended method for the analysis of self-similarity is the calculation of the variation of Rescaled Range (R/S) over different time scales of the data set. The R/S of a data set X(t) is defined over a period t as:

$$[R/S](\tau) := \frac{\max_{1\le k\le \tau}\{W_k\} - \min_{1\le k\le \tau}\{W_k\}}{\sqrt{\langle X^2\rangle_\tau - \langle X\rangle_\tau^2}} \qquad W_k := X_1 + X_2 + \ldots + X_k - k\langle X\rangle_k$$

If X(t) is self-similar, R/S(τ) will evolve with τ as $\alpha\ \tau^H$, where H is known as the Hurst parameter. The value of this parameter indicates the character of long term correlations: if H > ½, it indicates positive correlation (meaning persistence, or "long term memory" in the signal). If H < ½, it indicates negative correlation or antipersistence. In particular, the temporal mesoscale (defined in [9] as the range between the fluctuation characteristic times and the confinement time) is expected to show a persistent behaviour (H > ½). This is the case in all the above mentioned experiments, with H parameters between 0.6-0.7. A representative R/S(τ) curve of LHD camera signal (sample in the significative point in figure 3.1) during a high β (<β> =

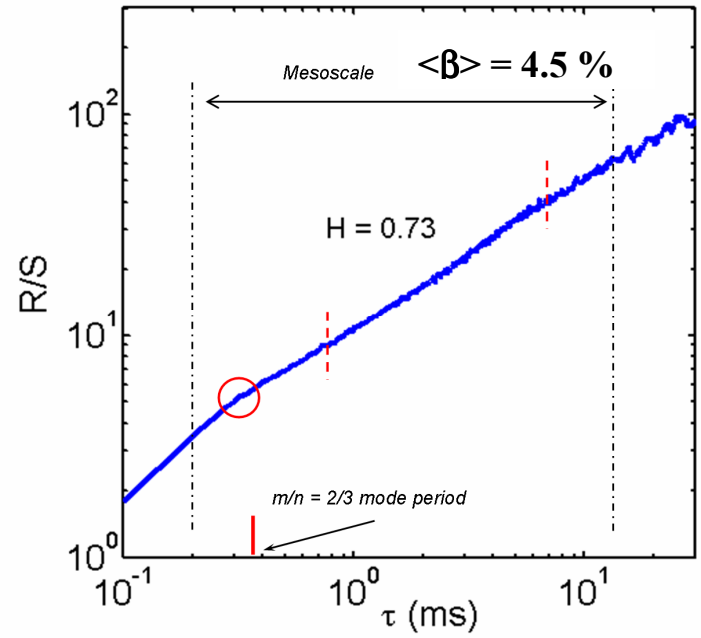

Fig. 3 *R/S(τ) analysis of a typical high b discharge from LHD. In self similar signals, Hurst parameter is measured as the slope of the curve. In this case, the mesoscale (between vertical black lines) includes the region influenced by the m/n = 2/3 mode (marked as red solid line) and the persistent region between red dashed lines, with H = 0.73.*

4.5%) discharge can be seen in figure 4, with the mesoscale noted by black vertical dashed bars. In it, it can be seen how the value of the Hurst parameter of the upper mesoscale is (region between red dashed bars) around 0.7, meaning a significative self-similar, persistent behaviour which lasts about one decade. The flat region of the lower mesoscale and the knee (marked with the red circle) preceded by a steep gradient can be explained as the result of a regular sinusoidal activity. In particular, the period of the aforementioned regular component of the signal associated to the m/n = 2/3 edge coincides nicely with the knee (marked in red). In conclusion, a first R/S analysis shows that fluctuations show a strong self-similarity on their behaviour, and that Hurst parameter evolution with time lag is consistent with that considered characteristic of avalanches in the SOC paradigm. The small variation on lower time scales can be easily explained by the presence of a strongly coherent mode, responsible for the lower frequency band of the structure propagation. As well, consistency with similar analysis performed in many other machines is reached. The physical interpretation of this would be the existence of some complex interaction between the release of particles associated to the mode and some degree of autoorganization of the transport, such as the development of SOC on the g-mode turbulence. These mechanisms would produce macroscopic releases of particles on the separatrix which would travel through the ergodic layer to the divertor leg. Due to their size, these releases would generate visible structures, such as filaments, which would conserve their coherence during the travel and therefore would retain their self-similar statistical properties on their ejection pattern. Still, these results can not be considered a conclusive proof of the presence of avalanches in LHD: a more complete analysis, including a systematic comparison of several indicators usually associated to SOC (R/S, waiting time distributions, fluctuation pdf tails, etc.), is still under way and will be addressed in future works. Finally, the role of $<\beta>$ on these mechanisms and its eventual implications on transport is to be investigated.

[1] M. Shoji, A. Iwamae, M. Goto et al, J. Nucl. Mater., 363-365 (2007), 827-832
[2] M. Goto and S. Morita, Plasma and Fusion Research, 2, S1053 (2007)
[3] S. Sakakibara, K. Watanabe *et al*. Plasma Phys. Control. Fusion, 50 (2008)
[4] D. Carralero, M. Shoji, E. de la Cal et al, Cont. Plasma Phys. in press
[5] P. Bak et al, Phys. Rev. Lett. 59, 381 (1987)
[6] D.E. Newman et al., Phys. Plasmas 3, 1858 (1996)
[7] D. del-Castillo-Negrete, Phys. Rev. Lett., 94, 065003 (2005).
[8] H. Funaba et al., Fusion Sci. Technol., 51 129, (2007)
[9] B.A. Carreras et al., Phys. Rev. Lett. 80, 4438, (1998)
[10] B.A. Carreras et al., Phys. Plasmas 6, 1885, (1999)